Geomorphology 319 (2018) 103–116

Contents lists available at ScienceDirect

Geomorphology

journal homepage: www.elsevier.com/locate/geomorph

Sedimentary records of extreme wave events in the southwestern Caribbean

L.Y. Puerres [a], G. Bernal [a,*], M. Brenner [b,c], S.A. Restrepo-Moreno [a,b], W.F. Kenney [c]

[a] Departamento de Geociencias y Medio Ambiente, Facultad de Minas, Universidad Nacional de Colombia Sede Medellín, Colombia
[b] Department of Geological Sciences, University of Florida, P.O. Box 112120, Gainesville, FL 32611, USA
[c] Land Use and Environmental Change Institute, University of Florida, P.O. Box 112120, Gainesville, FL 32611, USA

ARTICLE INFO

Article history:
Received 7 March 2018
Received in revised form 25 June 2018
Accepted 3 July 2018
Available online 11 July 2018

Keywords:
South Caribbean storms
Beach ridges
Coastal sediment records
Foraminifera

ABSTRACT

High-energy events in the Caribbean Sea include hurricanes, tropical storms, cold fronts and tsunamis. El Rosario Archipelago, located on the Colombian Caribbean shelf (SW Caribbean) consists of a set of ancient and successive coralline formations, uplifted by tectonic and diapiric activity. We undertook an integrated analysis of instrumental climate records and sediment records from a beach ridge system, a reef lagoon and a mangrove lagoon in the Archipelago, to determine whether historical extreme weather events influenced the coastal geomorphology and reef sedimentation. Statistical analysis of historical extreme winds and waves was accomplished using ERA-Interim reanalysis data. Extreme sea-level events were identified with calibrated data from the nearest tide gauge. Sediments from the reef and mangrove lagoon were dated using ^{210}Pb and ^{14}C. Beach ridges were dated indirectly thorough their relationship with the closure of the mangrove lagoon. The eroding capacity of the historical extreme waves (i.e. maximum grain size that could be entrained by the orbital velocity of the waves) was compared with the grain sizes present in the deposits, and foraminifera species helped to determine the provenance of those deposits. Storms typically occur during the dry season associated with cold fronts. Foraminifera and coral fragments indicated that beach ridges were supplied with sediment that eroded from ancient terraces. In the reef lagoon, a 56-cm-thick unit of coarse coral and shell debris, grading to a finer sediment, represents a major high-energy event that occurred after ca. 1655 CE. This event was also recorded by the beach ridges. The probable explanation for this high energy unit is that a strong event carried coarse sediments into the lagoon, with subsequent reworking by minor events, such as those reported in the historical record. Two tsunamis occurred in the Caribbean after 1655, but the associated waves reaching the area were not strong enough to deposit the coarser clasts of the unit. Thus, coarser material was probably delivered to the lagoon as a consequence of sudden diapiric and/or tectonic activity. Our data show that major storms and other high-wind, extreme-wave events shape the beach ridges on Rosario Island, every 70 years. The findings suggest that if global climate change increases the frequency and/or magnitude of major storms and other high-wind, extreme wave events that impact the Caribbean coast of Colombia, then El Rosario Archipelago will be susceptible to future, significant landscape transformations.

© 2018 Elsevier B.V. All rights reserved.

1. Introduction

There is growing consensus that future climate changes will be accompanied by an increase in the frequency and/or intensity of extreme weather (Sura, 2011; Ebi and Bowen, 2016). Changes in the strength of high-energy oceanic events not only affect coastal geomorphic processes (Coco et al., 2014; Houser et al., 2015; Houser et al., 2008), but also the abundance, distribution, morphology and behavior of species in ecosystems (Easterling et al., 2000), and hence human communities (IPCC, 2014). Extreme-event impacts on coastal communities include flooding, infrastructure loss, damage to crops and mariculture operations, and loss of ecosystem services. To better understand the consequences of extreme events, it is necessary to collect information from several ecosystems at multiple spatio-temporal scales (Jentsch et al., 2007). Studies of multiple sites in a region enable comparisons and verification of findings. One challenge associated with the analysis of extreme climate events, however, is the lack, or poor quality, of instrumental data extending beyond ~100 years ago (Easterling et al., 2000). Therefore, information on past extreme events, which is preserved in natural archives such as in coastal sediments, is essential to reconstruct the timing and magnitude of high-energy oceanic events over the long term.

Paleotempestology has focused primarily on the study of prehistoric tropical cyclone events. Inferences are derived from sediment records affected by the action of swells and/or waves (Nott, 2004). Cyclone events can be recorded in coastal sedimentary environments, including

* Corresponding author.
E-mail address: gbernal@unal.edu.co (G. Bernal).

https://doi.org/10.1016/j.geomorph.2018.07.002
0169-555X/© 2018 Elsevier B.V. All rights reserved.

beach ridges and lagoons. Beach ridges are sensitive indicators of changes in past sea level and coastlines (Otvos, 2000; Tamura, 2012). When beach ridges contain fragments of corals, shells and coarse sand, they enable the reconstruction of tropical cyclone chronologies and paleoenvironments at the millennial scale (Forsyth et al., 2010; Nott, 2004). Sediment cores provide additional and valuable information related to historic sedimentation and environmental changes on the seabed. Coastal or reef lagoons are environments where sediment records are often preserved, yielding evidence about past extreme oceanic events (Bourrouilh et al., 2007, Hawkes and Horton, 2012, Klostermann et al., 2014, Braun et al., 2017).

Extreme high-energy events in the Caribbean Sea include hurricanes, tropical storms, cold fronts and, less frequently, tsunamis. Approximately 1000 tropical storms and 200 category 2–5 hurricanes were registered in the Intra-American Sea during the last 100 years (Scheffers et al., 2009). Even though the Colombian coast is relatively sheltered from hurricane effects (Fig. 1), cyclone activity in the Caribbean has produced extreme waves that affected marine ecosystems (Bernal et al., 2016). Ortiz-Royero (2007) reported that 57 storms entered the southwestern Caribbean between 1900 and 2007, and several storms, such as Joan (1988), Bret (1993) and Cesar (1996) struck the Colombian Coast. Tropical storms and hurricanes in the Caribbean occur mainly between June and November. September and October are the most active months and coincide with Colombia's wet season. Nevertheless, extreme waves in the zone are most frequent during the dry season (December to April), as a result of enhanced activity of the Caribbean Low Level Jet (CLLJ) and the passage of cold fronts (Devis-Morales et al., 2017). About six cold fronts occur each year during the first three months of the dry season, and the most substantial extreme wave event of the last two decades in the Colombian Caribbean corresponds to a cold front that occurred in March 2009 (Ortiz-Royero et al., 2013). Tsunami effects on the Colombian Caribbean Coast are poorly understood (Lander et al., 2007). They appear to be less significant in magnitude, probably as a consequence of source location, regional propagation or local conditions (Caicedo et al., 1996).

Reefs from the El Rosario Islands Archipelago (ERIA), located on the Colombian Caribbean shelf, have been subjected to extreme wave events of different origins. Furthermore, the oceanographic setting of the ERIA constitutes a natural laboratory in which to obtain late Holocene sediment records that reveal past climate and environmental conditions in the region. To understand the impacts of the past extreme wind, wave and sea level events on the geomorphology and sediments in this area of the Caribbean Sea, we studied a beach ridge system located on Rosario Island, and sediments from the Pajarales Reef Lagoon and a mangrove lagoon. We explored the history of extreme oceanic events in the Archipelago by comparing records from these natural paleoenvironmental archives with instrumental records.

2. Study area

The ERIA (Figs. 1, 2) is located 52 km southwest of Cartagena Bay, on the north coast of Colombia. This archipelago rests on the continental

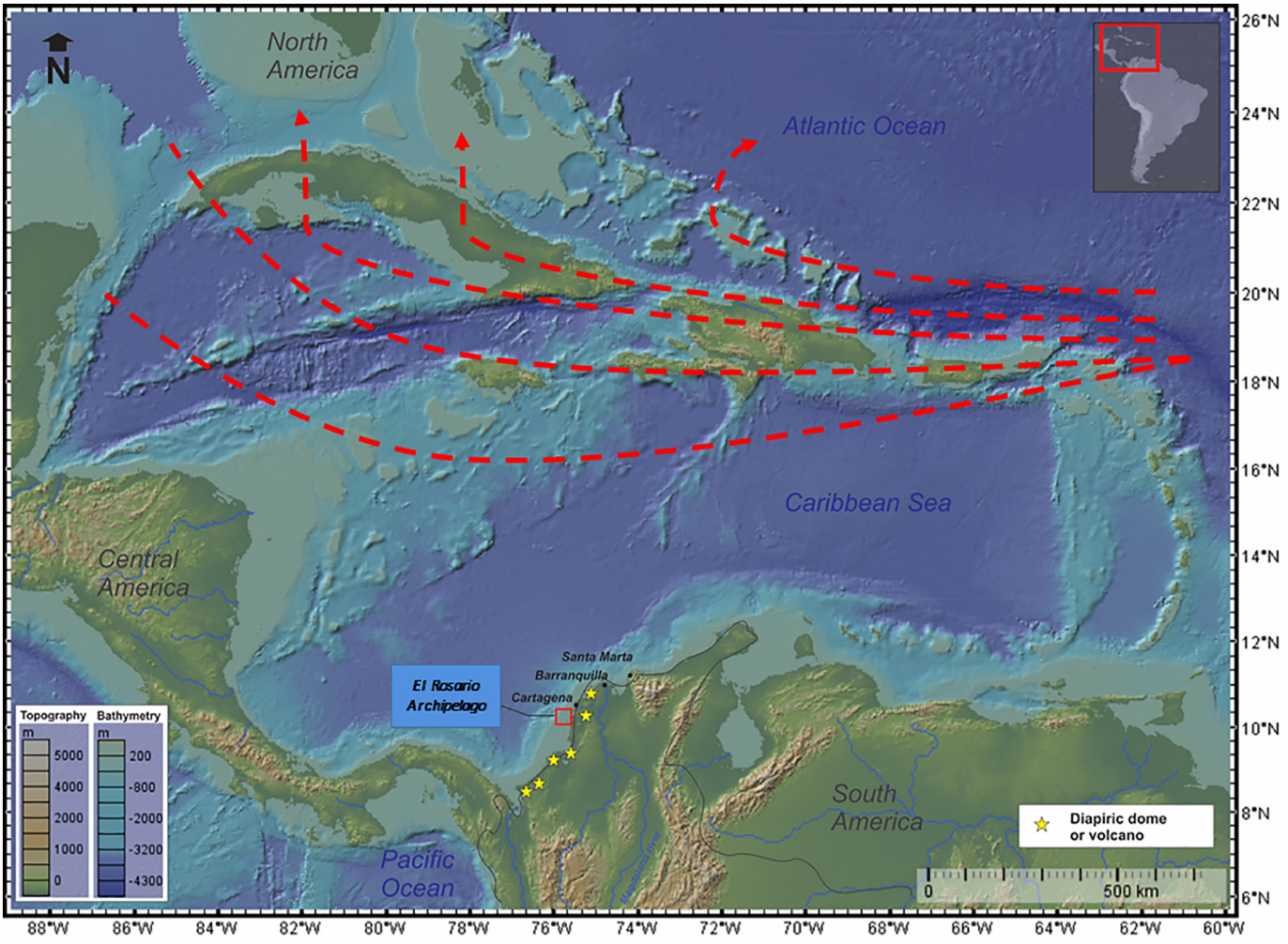

Fig. 1. Location of the "El Rosario Islands" Archipelago (ERIA), indicated by the red rectangle. Most probable hurricane paths for the Caribbean Sea are marked by red, dashed lines, and reported diapirs are indicated by yellow stars.

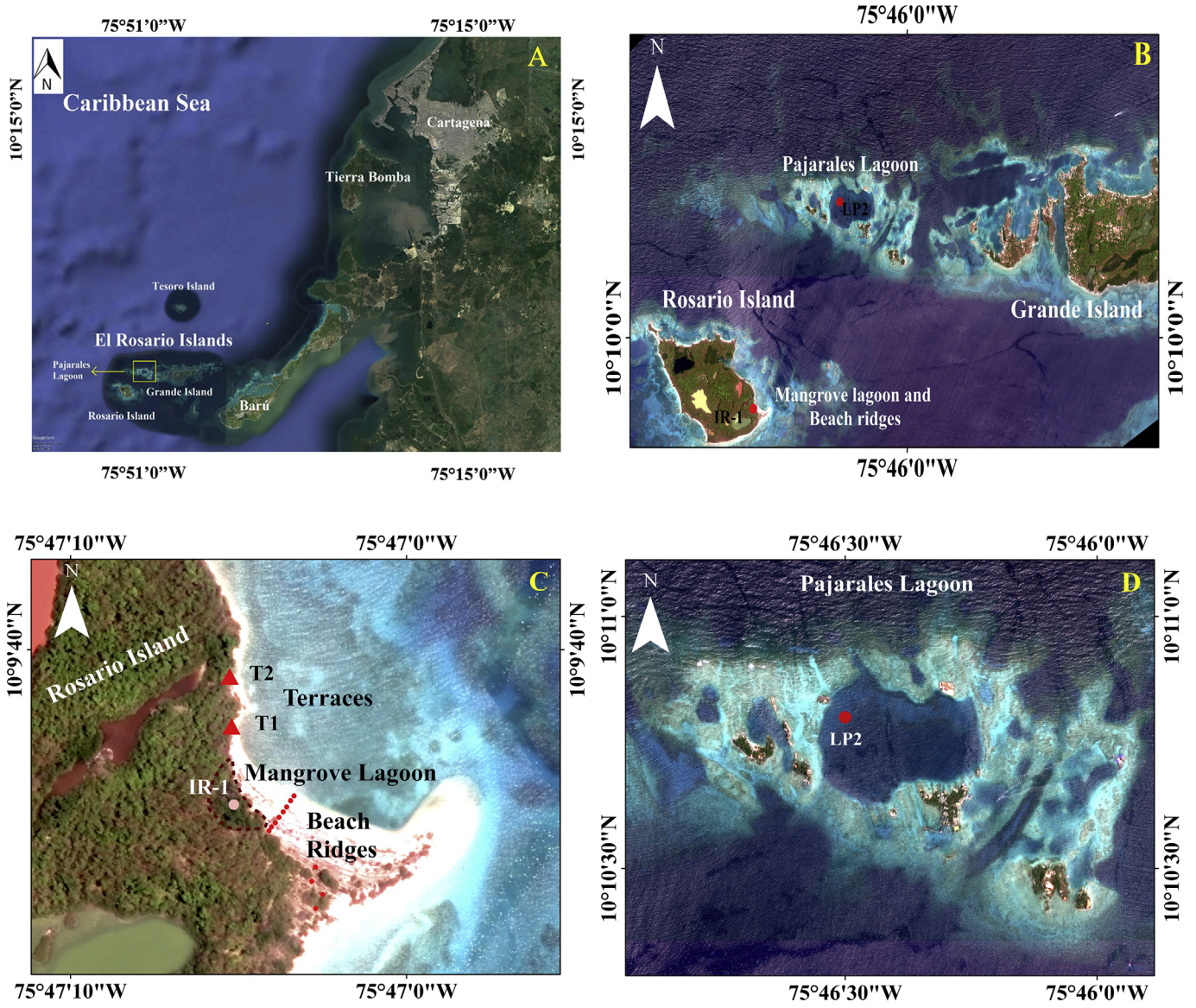

Fig. 2. Locations of the analyzed sediment records. A) Detailed location of the ERIA, SW of the city of Cartagena (image from Google Earth, downloaded December 2017). B) The main Islands of the Archipelago: Rosario Island, where this investigation was carried out, and Grande Island. C) Location of marine terraces (red triangles), core IR-1 in the closed mangrove lagoon (red circle) and beach ridges (small red dots), which collectively constitute the sampled locations along the southeastern shore of Rosario Island. D) Location of core LP2 in the Pajarales Lagoon.

shelf that marks the southern boundary of the Colombia Basin (Tomczak and Godfrey, 1994). Since 1977, the area has been legally protected as part of the "Corales del Rosario and San Bernardo National Park," which covers about 420 km^2 (Restrepo et al., 2012; Díaz et al., 2000). The ERIA includes 28 islands and cays built upon a set of ancient and successive coralline formations currently lying at least 3 m above mean sea level (Cendales et al., 2002). Most coral formations emerged in the middle Holocene, ca. 5000 years ago, forming the substrate of the islands (Díaz et al., 2000). The origin of the ERIA is linked to tectonic activity associated with the development of the Sinú-San Jacinto Folded Belts, at the transition between the Caribbean and the South American plates, a lithotectonic milieu characterized by folding/faulting of Paleogene-Neogene sedimentary successions, a process often accompanied by the development of diapirism and mud volcanoes (Restrepo et al., 2013; Vernette, 1978). Tectonic and diapiric activity are strong determinants of the region's geomorphology both inland and in the ocean. For example, Cendales et al. (2002) attributed the formation of the ERIA to Pleistocene-Holocene uplift related to a combination of tectonics and diapirism, which elevated the continental shelf to the photic zone, enabling the development of coral structures. During that period, relative sea level fluctuations caused the formation of several marine terraces with coral in the original position. Such terraces are found throughout the Colombian coast. Martínez et al. (2010) reported that terraces on Tierra Bomba Island date to between 2260 and 2020 BP. Although coralline terraces of the ERIA have not been directly ^{14}C-dated, it is thought that the similar geomorphic structures on Tierra Bomba Island provide a comparable age, given their geographic proximity and similar geodynamic environment.

The modern geomorphology of the ERIA is considered to be a result of sea level oscillations, reef accretion, and karstic processes (Díaz et al., 2000). Rosario Island is the second largest in size (Fig. 2B). In the Park's environmental management plan, all human activities are prohibited in this island. Vegetation consists of dry forest, mangroves and beach plants (Galeano et al., 2017). Some small lagoons inside the island have been attributed to karstic origin. The coastal zone is elevated on the eastern flank of the island, composed of cliffs on marine terraces and small bays with mangroves and beaches. The western flank has low coasts fringed by beaches. In the southeastern part of the island, a beach ridge system was deposited, enclosing a small mangrove lagoon

that was once connected to the ocean (Fig. 2C). Pajarales Lagoon (Fig. 2B and D) is a 20-m-deep depression surrounded by small cays and reefs. This area is protected from the direct action of waves and possesses the finest-grain sediments in the Archipelago.

Modern marine dynamics around the ERIA, and in the Colombian Caribbean in general, are influenced by the intensity and seasonality of the trade winds, forced by the migration of the Intertropical Convergence Zone (ITCZ) and linked to the CLLJ (Poveda et al., 2006; Andrade and Barton, 2000; Restrepo et al., 2012; Ruiz Ochoa et al., 2012; Beier et al., 2017). The December to April dry season is associated with strong trade winds and swells. Otherwise, high-energy extreme events in the Colombian Caribbean have been associated with hurricanes, extreme dry seasons, mid-summer droughts, and northern hemisphere winter cold fronts (Bernal et al., 2016). During the rainy season, from May to November, winds diminish, and riverine fresh water, along with abundant particulate material in suspension, advances over the shelf in the form of plumes (Cendales et al., 2002). These processes are associated with major fluvial systems such as the Magdalena River, the major contributor of fresh water and detrital materials to the Caribbean (Beier et al., 2017), and the El Canal del Dique, a distributary of the Magdalena River built in Colonial times and considered to be a major disruptor of natural fluvial-marine interactions in the ERIA (Restrepo et al., 2016).

At the sub-decadal scale, the Caribbean is influenced by the El Niño Southern Oscillation (ENSO). In Colombia, ENSO phases are linked to hydro-climatological anomalies that amplify the hydrological regime through complex and non-linear interactions. El Niño produces drier dry seasons, and La Niña wetter rainy seasons over the continent (Poveda et al., 2006). The Caribbean and Colombian fluvial basins, however, are affected by ENSO in different and complex ways. Rainfall over the Colombian Basin is not significantly related to ENSO, although salinity diminishes during La Niña and increases during El Niño, as a consequence of variations in river input (Beier et al., 2017). In addition, the CLLJ is stronger than normal during El Niño phases, and weaker during La Niña, especially during summer (Amador, 2008). Bernal et al. (2010) reported that winds over the Colombian Basin increase during the dry season in La Niña years, and during the wet season in El Niño years. During El Niño, positive sea surface temperature anomalies occur in the Caribbean (Enfield et al., 1999). Ruiz Ochoa et al. (2012) found that the inter-annual variability of sea surface temperature over the Colombian Basin was strongly related to the North Tropical Atlantic Index, a predictor of the development of El Niño and its influence on the Atlantic.

3. Methods

The methods deployed in this study combine two approaches: a) analyses of historical climatic-oceanographic series, and b) study of sediment and microfossil records.

3.1. Time series analyses

Time series of wind speed, wave height, and sea level were analyzed to identify recent extreme events in the ERIA. Wind and wave data were obtained from the ERA-Interim re-analysis (http://apps.ecmwf.int/datasets/data/interim-full-daily/levtype=sfc/; Dee et al., 2011), with a temporal resolution of 6 h and spatial resolution of 0.25° × 0.25°. Data span a range from January 1979 to April 2015. Sea level height was calculated from measurements taken in the ERIA with an RBR tide and wave logger between November 2013 and February 2014, and with a tide gauge located in the Bay of Cartagena, with data from 1950 to 2013 and 1-hour time resolution (http://uhslc.soest.hawaii.edu/datainfo/; Caldwell, et al., 2015). The overlapping time intervals between the two sea level series were compared and a correction factor was calculated to extend the series in the ERIA using the Cartagena tide series.

Statistical analysis of wind, waves and sea level extremes was carried out using R software (https://www.r-project.org/), by testing different probability distributions. Once the most appropriate distribution was selected, a threshold above 99% was defined to obtain extreme values for each series. Identification of events was undertaken following the "peak-over-threshold" method (Leadbetter, 1991). Extreme events for wave variables obtained from the ERA-Interim database were calculated in two segments, namely, before and after 1992, because since August 1991, the reanalysis began to assimilate satellite data which represents a significant change in the series (Dee et al., 2011).

3.2. Sedimentology

Sediment records were obtained from three settings in the ERIA (Fig. 2), including a reef lagoon (Pajarales), a set of beach ridges, and a mangrove lagoon (the last two located on El Rosario Island). Samples from coral terraces in El Rosario Island were compared with these sediment records for provenance. One sediment core (LP2, 86.5 cm long) was recovered from 20 m of water in the Pajarales Reef Lagoon. The LP2 core was collected by divers who used a coring device designed at the Hydraulics Laboratory (National University of Colombia in Medellín). A 2-m core (IR-1) was retrieved at Rosario Island from the mangrove lagoon that was closed by the beach ridge system. The IR-1 core was collected with a Macaulay Sampler. In addition, 12 beach ridges on Rosario Island were surveyed and sampled. Ten topographic profiles, perpendicular to the coastline, were surveyed in order to understand the succession of beach ridges. Ridge samples were collected by digging small trenches along the crests of the ridges, to depths between 25 and 30 cm. Lastly, with the aim of comparing and contrasting sedimentological material in terraces vs. ridges, six sediment samples from the terraces on the island were obtained from three strata. Sediments were discriminated based on coral species. LP2 was subsampled at 1-cm intervals, yielding a total of 87 sediment samples. IR-1 consisted of two sections. Uppermost deposits from 0 to 160 cm consist of peat that was subsampled every 2 (upper 10 cm) and 5 cm, yielding a total of 35 samples. Deeper material, from 160 to 200 cm, consists of sands that were sampled at 2-cm intervals, yielding a total of 20 sediment samples.

Excluding the peat section of IR-1, which consisted of >95% organic matter, all samples were analyzed for grain size following standard sedimentology procedures (McManus, 1988). Foraminifera were separated from the sand and conglomerate fractions using a stereomicroscope. Foraminifera abundances were very low in the terraces and beach ridges (<50 specimens per sample), but higher in the cores, where 100–300 specimens were counted per sample. According to Fatela and Taborda (2002), counts of 100 foraminifera individuals are sufficient to identify the dominant taxa, but they recommend counting 300 individuals to characterize the relative abundances for the total population. In the LP2 core, counting of foraminifera was done on 37 subsamples selected to characterize each unit. Benthic foraminifera were identified according to Loeblich and Tappan (1988), McCulloch (1977), Ellis and Messina Catalogues (1940–2014) and web sites such as the World Register of Marine Species (http://www.marinespecies.org/) and Foraminifera Gallery – illustrated catalog (http://www.foraminifera.eu/index.html).

Grain size and foraminifera data from IR-1 and the beach ridges were analyzed using correlation matrices and principal component analysis (PCA). Furthermore, organic matter and carbonate content ($CaCO_3$) in 35 samples from the LP2 core were measured by calcination (Darrel and Sommers, 1996) and calcimetry (Gaucher, 1971). The lithogenic fraction was calculated assuming that organic matter and carbonates account for the total biogenic fraction.

Eight peat samples from the mangrove lagoon (IR-1) from the surface down to a depth of 40 cm where unsupported ^{210}Pb disappeared, were used for ^{210}Pb dating. Analytical procedures for ^{210}Pb dating were performed at the Land Use and Environmental Change Institute (University of Florida, Gainesville). ^{210}Pb, ^{137}Cs and ^{226}Ra activities were measured by low-background gamma detection (Schelske et al.,

1994). Unsupported ^{210}Pb activity in each sample was determined by subtracting ^{226}Ra activity (i.e. supported ^{210}Pb activity) from total ^{210}Pb activity. We calculated sediment ages with the constant initial concentration (CIC) model (Robbins, 1978). For the CIC model, we estimated the average mass sedimentation rate (MSR, mg cm^{-2} a^{-1}) as the quotient of the decay constant of ^{210}Pb (0.031) divided by the slope of the regression of the natural log of unsupported ^{210}Pb against the mid-depth cumulative mass (mg cm^{-2}). We calculated age errors using the 95% confidence interval of that MSR estimate. Sediment ages were also calculated using the constant rate of supply (CRS) model (Appleby and Oldfield, 1983; Oldfield and Appleby, 1984). Age errors for the CRS model were propagated using first-order approximations and calculated according to Binford (1990). Ages and MSRs estimated by both the CIC and CRS models helped us constrain the linear sedimentation rate to optimize the fit of the chronological model to the ^{137}Cs peak (1964 CE) and the ^{14}C date for the base of the peat (1610 CE).

Radiocarbon (^{14}C) ages were determined on three samples (two foraminifera and one wood) from core LP2, two samples from the beach ridges (wood), and three samples from core IR-1 (one peat and two foraminifera from the sandy section). Samples were run by AMS at Beta Analytic (Miami, USA) and calibrated using the INTCAL13 database (Talma & Vogel, 1993; Reimer et al., 2013).

3.3. Eroding capacity of waves

To test whether historical events could have translocated sediments inside the lagoon, the wavelength (L) of waves reaching the ERIA was calculated from the mean peak period (Tp) of the wave series. Additionally the critical velocity for the movement threshold of the coarser sediments in the LP2 core and the orbital velocity of extreme waves in the historical record were calculated and compared. Critical velocity (Ucr) was calculated using the simplified formula of Van Rijn (www.leovanrijn-sediment, February 2017) for $0.0005 < d_{50} < 0.002$ m Eq. (2):

$$Ucr = 8.5(d50)^{0.6} * Log10\left(\frac{12h}{6d50}\right) \quad (2)$$

where h is water depth and d_{50} the median grain size of the sediment. Orbital velocity (Uorb) at this depth, for one of the most intense events in the historical record, was calculated using the formula proposed by Roelvink et al. (2015) Eq. (3):

$$Uorb = \frac{\pi H}{Tp * \sinh(kh)} \quad (3)$$

where H is the significant wave height, Tp is the peak period, h is depth, and k is the wave number obtained from the dispersion relation (Holthuijsen, 2007).

4. Results

4.1. Extremes of physical variables

Extreme winds were defined as winds with velocities > 10.15 m s^{-1} (Percentile 99 of Gumbel distribution). Forty-one extreme wind events occurred between 1979 and 2015. Four of these events displayed both high intensity and long duration, i.e. >6 h (Table 1). Two events (1 and 3) occurred during the dry season and were associated with cold fronts under La Niña or El Niño conditions. Occurrence of cold fronts was obtained from the Sea Weather Bulletin, published monthly by the Oceanographic and Hydrographic Research Center of the Colombian Army, CIOH, https://www.cioh.org.co/meteorologia). The other two events (2 and 4) occurred during the wet season and were related to the passage of two of the strongest hurricanes in Atlantic history, Lenny (1999) and Sandy (2012) (Guiney, 2000; Blake et al., 2013).

Extreme wave heights (Hs) were considered to be >1.57 m before 1992 and >1.75 m after 1992 (Percentile 99, Gumbel distribution). A total of 128 events were identified, and 16 were selected based on the combination of intensity and duration (Table 2). The most intense and enduring extreme events before 1992 occurred during the dry season, between the months of December and March, reaching the highest Hs value (1.9 m) in December 1991. It was not possible to identify the precise origin of the events during that period, because no CIOH Bulletins are available from that time. Extreme events between 1992 and 2015 were associated mainly with cold fronts in the dry season, and in the case of one, passage of a hurricane during the wet season (event 11, Hurricane Lenny). The maximum intensity of Hs, 2.4 m, occurred in January 2004 during the passage of a cold front.

Using a similar approach to identify the most significant sea level height extremes, 43 events were selected (not shown), with 28 of them (65%) occurring under El Niño conditions. Most events occurred during the wet season, coincident with hurricanes. Hurricane Joan (October 1988) made landfall on the Colombian coast and was associated with these significant sea-level height extremes. In the dry season, the strongest extreme event occurred in January 1983, under El Niño conditions, but no information about the specific climate conditions associated with this event (e.g., a cold front) was found.

4.2. Sedimentological variables

Core LP2 in Pajarales Lagoon consisted primarily of calcareous sand (Fig. 3). From bottom to top, four main segments were identified. Unit 1 (86.5–60 cm), displayed poorly sorted, coarse sand with some coral fragments up to 3 cm long. From 60 to 30 cm (Unit 2) the dominant components were very poorly sorted, very coarse sands, with abundant coral fragments 1–2 cm long and bivalve shells with diameters > 2 cm. Unit 3, between 30 and 4 cm depth, showed deposition of poorly sorted medium sands up to 5 cm depth, followed by 1 cm of fine sand (5–4 cm). The upper stratum, Unit 4, extended from 4 to 0 cm and consisted of poorly sorted medium sands. From all the levels examined, unit 3 presented the highest mud (clays and silts) content, up to 25%, compared to values of about 15–18% in the other units. Units 2 and 3 (Fig. 2) correspond to a high energy event, because of their high fragment content and gradation to finer sediments (mean size 0.250 mm, with 22% mud) at the top of the unit 3. The radiocarbon date for the deepest sample (86–85 cm) in the LP2 core is 1700 cal years BP (cal 250 CE). Units 2 and 3 yielded "inverted" ages with the deeper sample from 40 to 39 cm having a younger age (cal 1655 CE) than the shallower (26–25 cm) one (cal 905 CE), indicating probable mixing. The event that caused such mixing should have occurred after ca. 1655 CE.

LP2 had benthic foraminifera abundances between 97 individuals/g (ind/g) at the base, and 437 at 5 cm depth. Foraminifera abundances generally increase toward the top, with a significant abundance peak

Table 1
Strongest and longest extreme wind events that occurred in the ERIA between 1979 and 2015. Dates for onset and end of the events are d/m/yr and hour.

Wind event number	Onset of event	End of event	Duration (hours)	Wind speed (m s^{-1})	Observations
1	12/03/1996 18:00	13/03/1996 0:00	6	10.325	Niña condition/cold front
2	15/11/1999 12:00	16/11/1999 0:00	12	11.016	Hurricane Lenny (category 5)/Niña condition
3	08/03/2010 0:00	08/03/2010 12:00	12	11.796	Niño condition/cold front
4	24/10/2012 18:00	25/10/2012 0:00	6	11.672	Hurricane sandy

Table 2
Highest and lowest-duration extreme wave events that occurred in the ERIA between 1979 and 2015. Dates for onset and end of the events are d/m/yr and hour.

Wave event number	Onset of event	End of event	Duration (hours)	Hs_max (m)	Observations
Extreme events of significant wave height (Hs) from 1979 to 1991					
1	31/03/1979 6:00	02/04/1979 6:00	48	1.8	Normal condition dry season
2	14/01/1981 0:00	14/01/1981 12:00	12	1.8	Normal condition dry season
3	24/03/1986 0:00	24/03/1986 12:00	12	1.7	Normal condition dry season
4	10/02/1987 0:00	10/02/1987 12:00	12	1.8	Niño condition dry season
5	29/01/1988 0:00	30/01/1988 12:00	36	1.8	Niño condition dry season
6	25/02/1989 6:00	26/02/1989 12:00	30	1.7	Niña condition dry season
7	11/03/1989 0:00	11/03/1989 12:00	12	1.7	Niña condition dry season
8	26/12/1989 0:00	26/12/1989 12:00	12	1.8	Niña condition dry season
9	22/12/1991 0:00	23/12/1991 6:00	30	1.9	Normal condition dry season
Extreme events of significant wave height (Hs) from 1992 to 2015					
10	12/03/1996 6:00	13/03/1996 18:00	36	2.1	Niña condition cold front
11	15/11/1999 18:00	16/11/1999 12:00	18	2.2	Niña condition Hurricane Lenny (category 5)
12	16/01/2000 18:00	17/01/2000 12:00	18	2.4	Niña condition/cold front
13	06/02/2009 0:00	07/02/2009 12:00	36	2.1	Normal condition cold front
14	07/03/2009 0:00	08/03/2009 6:00	30	2.3	Normal condition cold front
15	08/03/2010 0:00	08/03/2010 18:00	18	2.1	Niño condition cold front
16	15/12/2010 0:00	15/12/2010 18:00	18	2.1	Niño condition cold front

at the top of the high energy unit (5 cm depth). Foraminifera abundances in the upper unit are between 200 and 250 ind/g. Foraminifera fragments were more abundant in Unit 2. Foraminifera from three suborders were found, with Textulariina the most poorly represented. The most abundant taxa were *Amphistegina lessonii* (22%), *Quinqueloculina lamarckiana* (11.9%), *Textularia agglutinans* (9.7%), *Quinqueloculina agglutinans* (6.7%) and *Amphistegina radiata* (5.8%). *A. lessonii* predominated in unit 1 (41%), *A. lessonni*, *Q. lamarckiana* and *T. agglutinans* in Units 2 and 3 (>90%), and *Q. agglutinans* and *Q. lamarckiana* in Unit 4 (>50%). Some foraminifera of the genus *Amphistegina* were highly calcified, weathered and fragmented, and were found throughout the whole LP2 core (total abundance 2.8%). These individuals may come from the

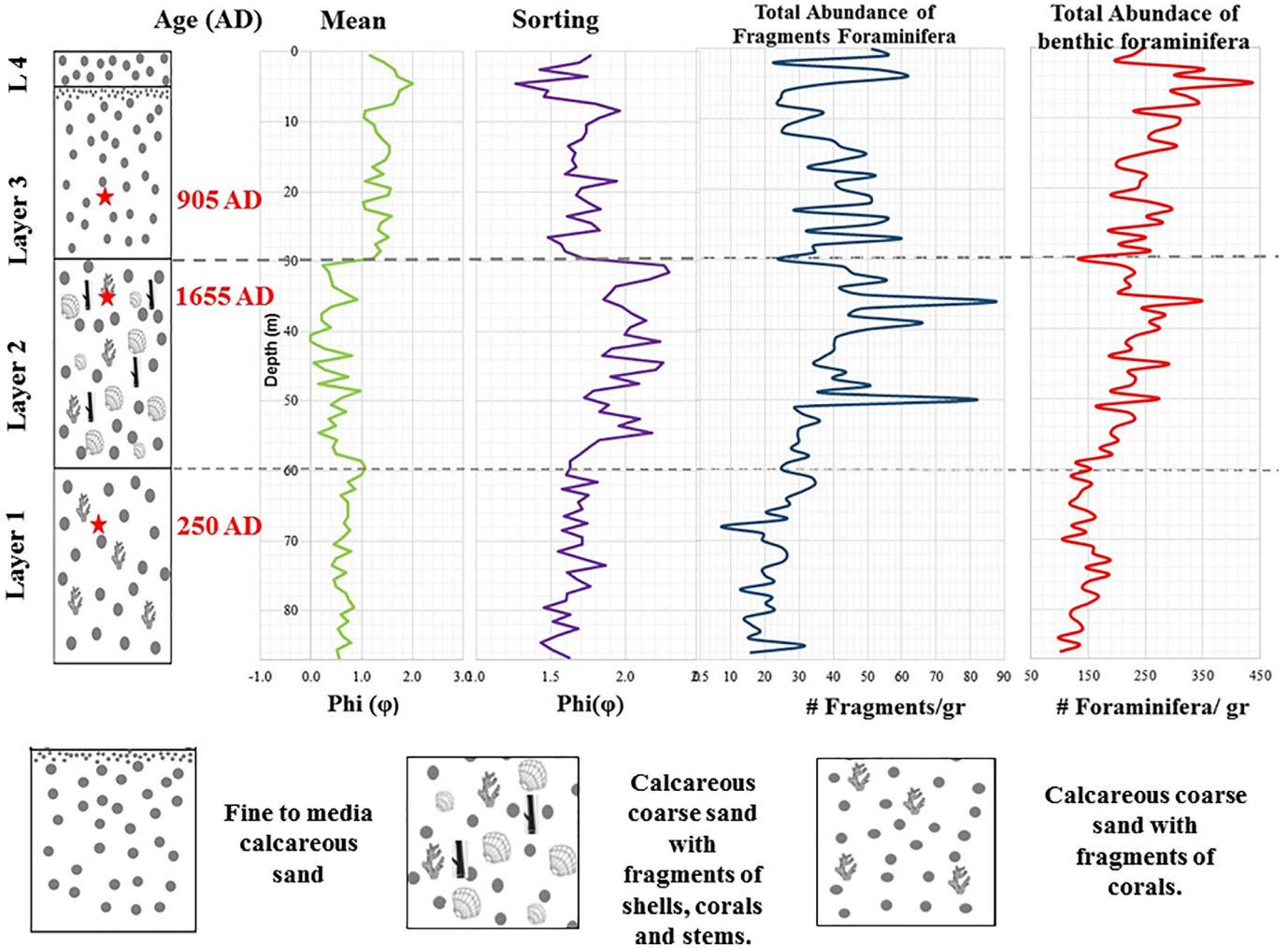

Fig. 3. Grain size distribution and ^{14}C dates for the Pajarales Lagoon Core (LP2).

island terraces and can be considered fossils. We refer to this taxon as *Amphistegina sp1*.

Carbonates ranged between 75 and 95% of sediment dry weight (mean 83%). Organic matter was low, with a mean value of 3.4%, increasing toward the top. Terrigenous sediment, i.e. non carbonate inorganic material, was greatest in Unit 3 (12.5–20%), lowest in Unit 4 (1.4–13%) and between 9 and 15% in Units 1 and 2.

Table 3 shows the average values of these variables in each unit.

Core IR-1, from 2.0 to 1.67 m, was made up of calcareous material, followed by 7 cm of a mixture of calcareous material and peat, and finally, the upper 1.60 m was a dark brown peat. The closure of the small mangrove lagoon where Core IR-1 was retrieved is marked by the transition from calcareous material to peat. Size analysis of the calcareous portion (Fig. 4) indicated very poorly sorted sands, very coarse at the base and medium toward the transition zone.

The chronological model for the peat section obtained by combining a ^{14}C age at the base of the peat with ^{210}Pb dates from the upper part of the IR-1 core is indicated in Fig. 4. At the base of the peat, near the transition to calcareous sands (158–156 cm), ^{14}C yielded a date of AD ~1610 ± 30. For the calcareous fraction (176–170 cm and 168–164 cm) ^{14}C ages were not measured because $\delta^{13}C$ of foraminifera shells showed fresh-water conditions (−6.5 and −11.3‰).

In the peat section, unsupported ^{210}Pb activity decreased with depth from 10 cm to 40 cm. Unsupported ^{210}Pb activity, however, increased with depth in the uppermost 10 cm of the core. A constant linear sedimentation of 0.46 cm yr^{-1} was similar to the mean sedimentation rate determined by the CIC model, and had an optimal fit with both the reference age of 1964 CE for the ^{137}Cs peak, and the ^{14}C date for the base of the peat, 1610 CE. Using this chronological model, closure of the lagoon occurred ca. 1657 CE.

Foraminifera in the calcareous section (20 samples) showed five abundance peaks, with the highest occurrence of foraminifera near the transition from calcareous sediment to peat (Fig. 5A). Seven species dominated the record (Fig. 5B): *Ammonia tepida*, *Ammonia beccarii*, *Trochammina inflata*, *Ammonia limnetes* and *Arenoparrella mexicana*, *Discorbis* sp., and *Amphistegina sp1*, the fossil variety of *Amphistegina*. Above 188 cm, however, *Ammonia tepida* was five times as abundant as other species (250–1050 ind g^{-1}). This species was responsible for the abundance peak that occurs in the transition, where maximum abundance was reached. The Shannon-Wiener Diversity Index values were >2 below 188 cm, but <2 above this depth, indicating the dominance of this species in the top of the calcareous section, and especially during lagoon closure.

There was a negative correlation between *A. tepida* and *D. sp1* ($r = -0.79$) and diversity (Shannon index, $r = -0.87$), but a positive correlation between *A. tepida* and total abundance ($r = 0.63$). Diversity was positively correlated with *A. beccarii* ($r = 0.53$), *A. limnetes* ($r = 0.72$) and *D. sp1* ($r = 0.83$), but negatively correlated with mean grain size ($r = -0.58$). All the above correlation values are significant at $p < 0.05$. Negative correlation between diversity and mean grain size in phi units indicates that diversity is higher in coarser sediments. *A. tepida* was very abundant in fine sediment, decreasing diversity. PCAs applied to foraminifera species showed four components explain 88% of the variance. PC1: Highly correlated with *A. tepida*, *A. limnetes*, *T. inflata*, *A. sp1* and *D. sp1* (*A. tepida* abundances vary inversely with the other species). PC2: Dominated by *A. beccarii*, *T. inflata*, *A. mexicana* and *A.sp1*, (*A. beccarii* and *A. sp1* vary inversely with agglutinated species *T. inflata and A. mexicana*). PC3: *A. beccarii* and *A. mexicana*. PC4: Dominated by *A. tepida*.

Table 3
Average organic matter, carbonate and terrigenous (non carbonate inorganic) material in units of LP2.

Unit	Average organic matter (%)	Average carbonates (%)	Average terrigenous (%)
4	4	89.2	6.8
3	3.6	80.3	16.1
2	3.1	83.7	13.3
1	3	83.6	13.4

Beach ridges consisted of poorly sorted pebbles of reworked coral fragments and shells (bivalves and gastropods), with a sand-size matrix of the same composition. Ridges were parallel to the coastline, but discontinuous. The oldest ridges (R12 to R9) were better consolidated, higher and broader than the younger ones (R8 to R1), but they also displayed higher erosion. A generalized topographic profile of sampled ridges is shown in Fig. 6. The profiles were more elevated toward the coastline. There was a gap between R6 and R5, Ridge R6 is just in front of the small closed lagoon where core IR-1 was collected.

Benthic foraminifera abundances in the beach ridges were 12–51 ind g^{-1}. Assemblages were dominated by nine species (Fig. 7). *Amphistegina lessonii* was the most abundant in all ridges, with a mean relative abundance of 49%. The agglutinated species *Trochammina inflata* occurred only in R8 and R6. Foraminifera assemblages changed before and after R8 (Fig. 7). Ridges between R12 and R9 display a Shannon diversity index < 2, but between R8 an R1 it is >2.

Parotalia nipponica and *Cymbaloporetta esquammosa* were present in the majority of ridges. These species were found in the terraces, which may indicate their provenance. Some specimens of the genera *Amphistegina* (*Amphistegina sp1*), *Quinqueloculina* and *Archaias* displayed fossil-like features such as high weathering, calcification, and fine sediment fillings, indicating that shells come from old terraces (T1 y T2) that form the cliffs of the island (Fig. 8). Coral fragments from ridges and terraces shared the same features, indicating a similar origin, though many of the found species (*Porites astreoides*, *Agaricia* cf. *tenuifolia*, *Agaricia* cf. *agaricites*, *Diploria labyrinthiformis*, *P. divaricata*, *Orbicella*, sp., *Acropora cervicornis*, *Meandrina meandrites*, *Stephanocoenia intersepta*) are also abundant in modern reefs.

Diversity in beach ridges correlated negatively with *R. globularis* ($r = -0.6$) and positively with other species. Foraminifera fragments exhibited a positive correlation with *Q. agglutinans* (r = 0.6), *Q. tricarinata* (r = 0.7) and *P. inornata* (r = 0.7), all of which belong to the *Miliolina* suborder, which is characterized by its sturdiness and adaptation to high-energy environments (Boltovskoy and Wright, 1976). Significant correlation was not found between *T. inflata* and other species or sedimentological variables. PCA of foraminiferal species indicated that four components explained 77% of the variance. PC1 was dominated by *R. globularis*, *C. squammosa*, *Q. lamarckiana*, *N. terquemi*, *P. inornata* and *P. mediterranensis*. Relative abundance of *R. globularis* was negatively correlated with the other taxa.

Direct dating of beach ridges was not possible. Radiocarbon analyses were run on two wood fragments from R12 and R6 (30 cm depth), but results were post 0 BP, i.e. super modern. Therefore, ridges were dated indirectly, as closure of the mangrove lagoon coincided with R6 and according the age model of IR-1, occurred around 1657 CE. Thus, R5 to R1 were formed between 1657 CE and 2014, which indicates that the ridges had a mean formation interval of ca. 70 years.

4.3. Eroding capacity of waves

The half wavelength (L/2) of waves reaching the ERIA calculated from the mean peak period (Tp) of the wave series (6.1 s) was 29 m. It indicates the threshold depth at which waves can interact with the sea floor. In Pajarales Lagoon, with an approximate depth of 20 m, high-energy waves could interact with sediments on the sea floor.

Critical velocity (Ucr) to move the coarser grains deposited in Pajarales lagoon (0.55 mm) was 0.46 m s^{-1}. Values for H and Tp used in our calculations were 2.4 m and 9 s, respectively. The resulting Uorb value was 0.56 m s^{-1}. This means that extreme events such as those identified in the historical record from 1979 to 2015 could set coarse sediments of the tempestite in motion, and could suspend the finer fraction (particles < 0.3 mm could be suspended).

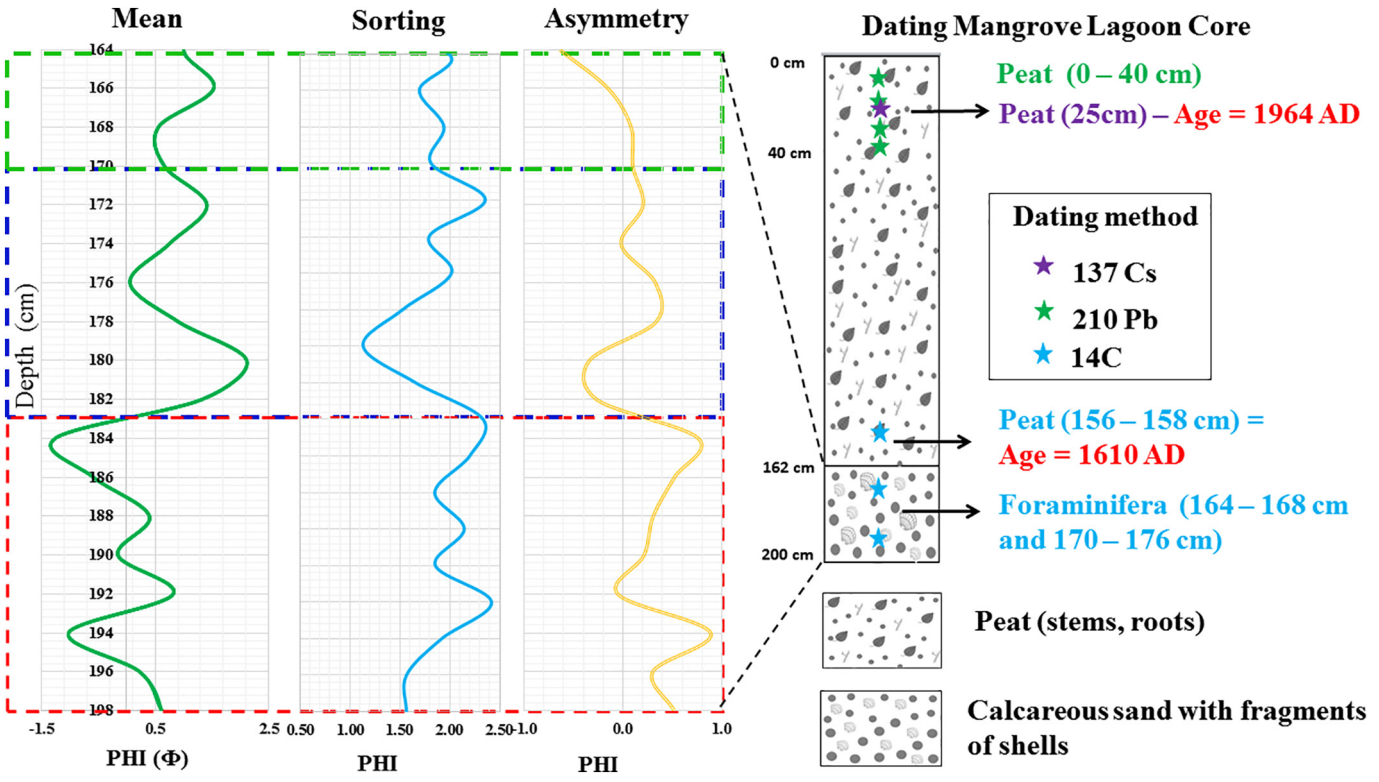

Fig. 4. Core IR-1 with details of grain size analysis of the calcareous portion (A) and dated samples (B).

5. Discussion

5.1. Linking the climate record with geomorphology

The strongest storms in the Caribbean Sea are related with hurricanes. The southwestern Caribbean, however, is relatively protected from hurricanes. The analysis of wind, waves and sea level in the ERIA confirm this. This analysis found that the strongest and longest wind and wave events there were related more with cold fronts (dry season) than with hurricanes (wet season). Only some hurricanes stood out for their impact on winds and/or waves, Lenny (1999) and Sandy (2012). Sea level extremes did not coincide with wind or wave extremes. They occurred mainly during the wet season in El Niño years. The only hurricane effectively related with an intense and long sea level extreme was Joan (1988).

According to Devis-Morales et al. (2017), in spite of tropical storms being a major climate feature in the Caribbean Sea that cause extreme metoceanic conditions, the coastal areas of Colombia are relatively sheltered from storm impact and the extreme events are more related to intensification of the CLLJ. Also, extreme events that occur during the wet season are shorter. In the Colombian Basin, high-sea-level events result from the steric effects of warmer waters (e.g. Ruiz-Ochoa et al., 2012) and hurricane-induced storm surges are rare (Torres and Tsimplis, 2014).

Major storms that recurred at intervals of ca. 70 years determined the formation of beach ridges on Rosario Island. Sediments that eroded from neighboring terraces constitute the main source of detrital material to beach ridges. Species of foraminifera such as *Cymbaloporetta squammosa* and *Pararotalia nipponica*, found in both, beach ridges and terraces, as well as coral fragments, indicated that these beach ridges were supplied with abundant sediments eroded from nearby terraces.

Beach ridges bear evidence of extreme wave events in other coastal regions of the world (Nott, 1997, 2004; Hayne and Chappell, 2001). Beach ridges reported from other locales exhibit formation periodicities between 15 and 270 years. Clemmensen and Nielsen (2010) assigned cycles of ca. 15 years to a series of beach ridges formed by storm waves in Kattegat Island, Denmark. Ridges in the Gulf of Mexico seem to exhibit a common frequency of formation of ca. 30–60 years (Tanner, 1995). Forsyth et al. (2010), Nott (2011) and Bendixen et al. (2013) refer to centennial scales for beach ridges in Australia and Denmark. Nevertheless, centennial-scale ridges are usually higher (6 m) compared to those in Rosario (0.4 m), which are typically associated with more frequent, less intense waves. The frequency of ridge development on Rosario Island is analogous to that of the Gulf of México, where similar oceanographic environments are identified, with maximum waves in the historical record (last 36 years) exhibiting heights of 2.2 to 2.4 m, and storm durations between 3 and 6 days. The 70-year, high-energy events that affected the ERIA should have had magnitudes at least this vast.

In the Caribbean, Morton et al. (2008) studied ridge complexes on Bonaire, Jamaica, Puerto Rico (Isla de Mona) and Guadeloupe, in an attempt to distinguish ridges formed by tsunamis from ridges associated with storm-waves. The ridge complexes studied in that work had crest heights between 2 and 3.5 m and their formation spanned centuries to millennia. The authors concluded that such ridges are the result of multiple, high-frequency extreme wave events, and that tsunami deposition may account for only some accretion of boulder fields or isolated blocks associated with the complexes. Because of their location, the deposits studied by Morton et al. (2008) are more susceptible to hurricanes and tsunamis than are those in the southwestern Caribbean. From this we infer that the beach ridges at Rosario Island were formed by storms, but are much smaller than the ridges studied by Morton et al. (2008) because of the secluded nature of this portion of the littoral zone of Colombia.

On Rosario Island, prograding beach ridges enclosed a small mangrove bay, converting it into a closed lagoon. Sedimentation in the lagoon analyzed using the IR-1 core, clearly showed its closure occurred around ca. 1657 CE. Before closure, sedimentation was predominantly calcareous; during closure, a mixture of calcareous material and peat occurred; and after closure, only peat accumulated.

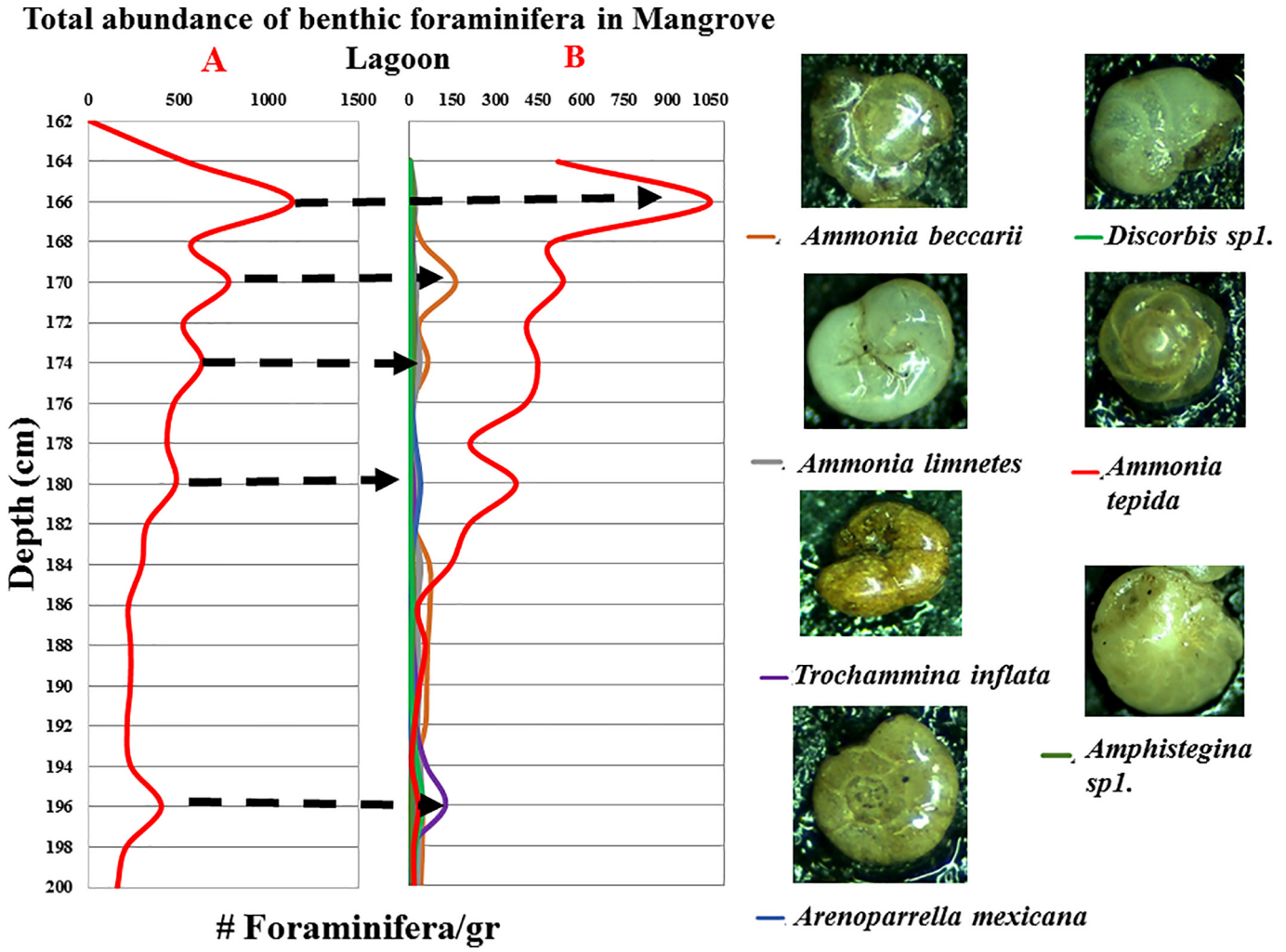

Fig. 5. Total abundance of benthic foraminifera in the calcareous section of IR-1 (A) and abundance of the most important species (B). The dotted lines mark abundance peaks showing how the total abundance of foraminifera coincides with the most abundant species peaks.

In the calcareous section of the IR-1 core, *Ammonia tepida* dominated the assemblage and displayed several periods of high abundance, the last occurring just before lagoon closure. The agglutinated species *Trochammina inflata* was found from the base to the closure of the lagoon, but its greatest abundances were recorded near the base of the core, at depths between 198 and 192 cm. *Trochammina inflata* prefers highly saline or brackish water bodies (Sen Gupta, 1999) that were characteristic of the open lagoon, with marked oceanic influence. *Ammonia beccarii* and *Ammonia tepida*, two species found in the IR-1 core, are typical in bodies of calm water, the difference being that *A. beccarii* prefers saline environments and *A. tepida* brackish environments (Almogi-Labin et al., 1995). This contrast explains the distribution of the two species, the former from the base to the middle of the section indicating more open marine conditions, and the latter, in the transition to lagoon closure indicating mainly brackish conditions. After the closure of the lagoon, foraminifera disappeared, only peat accumulated, and a stable freshwater environment was established. This inference is supported by the $\delta^{13}C$ values of foraminifera in the IR-1 core, which are typical for fresh-water conditions.

Before closure, foraminifera from the lagoon were supplied to beach ridges. *Amphistegina lessonii* was the most abundant species in all ridges. This is a common species throughout the archipelago (Puerres, 2016) and can come from the sea. Foraminifera assemblages in the beach ridges, however, changed before and after R8. *Trochammina inflata* occurred only in R8 and R6. This species is typical of mangrove environments, and was present in IR-1. Most probable provenance corresponds to the small bay that became the closed mangrove lagoon. The change in assemblages and the occurrence of *T. inflata* indicates that the closure of the lagoon started with R8 and terminated with R6.

Foraminifera documented in this study constrain sedimentologic processes related to high-energy events in the ERIA, as foraminifera assemblages are often used to estimate the provenance of tsunami and storm deposits. For example, deposits associated with Hurricane Ike (2008) were studied in Galveston and San Luis (Texas, US), with sediments and foraminifers indicating the origin of internal platform environments (Hawkes and Horton, 2012). Also, Pilarczyk et al. (2012) found that associations of foraminifera from the Tōhoku-oki tsunami, deposited on the coastal plain of Sendai (Japan) in 2011 came from coastal sediments of beaches and dunes, whereas others originated from intertidal environments. Hawkes et al. (2007) analyzed the 2004 Tsunami deposit in the Indian Ocean on the Peninsula of Thailand and argued that foraminifera were effective for distinguishing between syn-tsunami vs. pre-tsunami sediments. In addition, these planktonic associations provided information on sediment provenance from the internal platform and mangrove environments.

5.2. High energy layer formation

Sediments deposited during the last 1760 years (since 250 CE) in Pajarales Lagoon (87 cm in core LP2) showed a 56 cm section that can be classified as high energy according to the following evidence: (1) coarse grain size; (2) inverted ages, with younger sediments

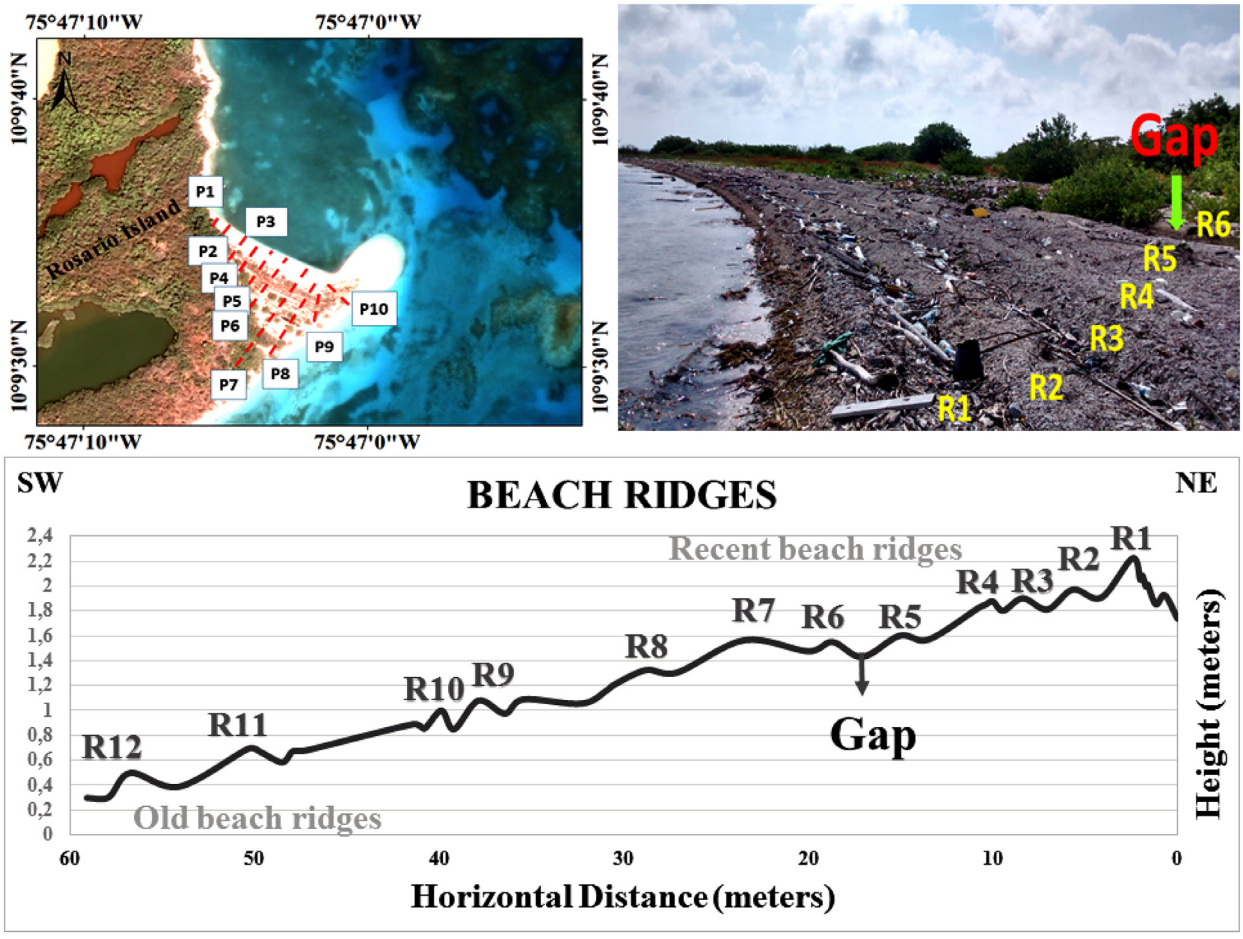

Fig. 6. Beach profiles surveyed and beach ridges on Rosario Island. P1 through P10 indicate the topographic profiles produced during the survey. R1 through R12 are the sequence of ridges investigated. Surveyed profiles over ridge structures are marked as P1 through P10 in the upper left figure.

below older ones; (3) larger clast sizes at the base, and gradation of sediment toward fine sands at the top; (4) higher benthic foraminifera content, possibly from allochthonous contributions; (5) increase in foraminifera fragments and weathered foraminifera in the coarser fraction (60–20 cm); (6) greater abundance of *Amphistegina sp1*, which may come from erosion of nearby cliffs.

The event that formed this unit probably occurred after 1655 CE. It is also feasible that there has been constant reworking of sediments during recurrent extreme weather events, such as those identified in the historical series. Extreme wave events reflected in the analyzed historical records possesses enough energy to have mobilized sediments at the bottom of the Pajarales Lagoon and suspend particles < 0.3 mm. The estimations can be higher or lower. On the one hand, ERA-Interim dataset can underestimate wave extremes in the Colombian Caribbean (Devis-Morales et al., 2017) increasing the probability of resuspension by annual extreme waves. On the other hand, the parameters of sediment movement were estimated with waves in open waters. The magnitude of wave dissipation by the reef around the lagoon is not known, and this effect could decrease the probability of resuspension of sediments in the lagoon by historical events.

In any case, it is unlikely that events of this magnitude produced the high energy unit. The most probable explanation for the development of this deposit is that a strong event carried coarse sediments into the lagoon and subsequent events of lesser intensity, such as those reported in the historical record, reworked the upper portions of the unit. These combined events produced the characteristic sorting and a chronological inversion of the sediment column.

The gap between beach ridges R6 and R5 occurred shortly after the closure of the small lagoon on Rosario Island, which took place around 1657 CE. This age is the same as that of the youngest dated sediments of the high energy unit (1655 CE) in Pajarales Lagoon. It means that it is probable that both the gap between the ridges and the tempestite-like unit were produced by the same event. Gaps in storm beach ridge plains can be attributed to intense erosion or to cessation of storm activity (Nott et al., 2015). Being synchronous with the high energy unit, the origin of the gap between beach ridges R6 and R5 on Rosario Island must reflect intense erosion.

It has proven difficult to distinguish between tsunamis and storm deposits in tempestite records from different parts of the world because the two processes can be superimposed in the sediment record (Brill et al., 2011). In the ERIA, the historical record for the last three decades displays no evidence of a meteorological event of sufficient magnitude to generate the thick deposit found in Pajarales Lagoon. Thus, an alternative explanation involves a tsunami. The strongest tsunami events recorded in the Caribbean, with possible impact in the Colombian coasts, are those of 1755, with the epicenter in the Lesser Antilles and Cuba, and 1867, with the epicenter in the US Virgin Islands, Guadalupe, Puerto Rico and Grenada (Lander et al., 2007). According to Caicedo et al. (1996) and Yandar and De la Cruz (2015), historical tsunami waves reaching the Colombian coast had heights of 1.0–2.6 m, i.e., a magnitude similar to the extreme waves documented in the historical record. The relatively low magnitude of tsunami waves reaching the Colombian coast explains why there are no reported sediment records associated with these tsunamis on the Caribbean coast of Colombia.

Unfortunately, with the information generated previously and in this investigation, it is not possible to constrain the age of the high energy unit or to attribute it to a distinct event. Triggering mechanisms are not necessarily related to climate, because an abrupt tectonic or

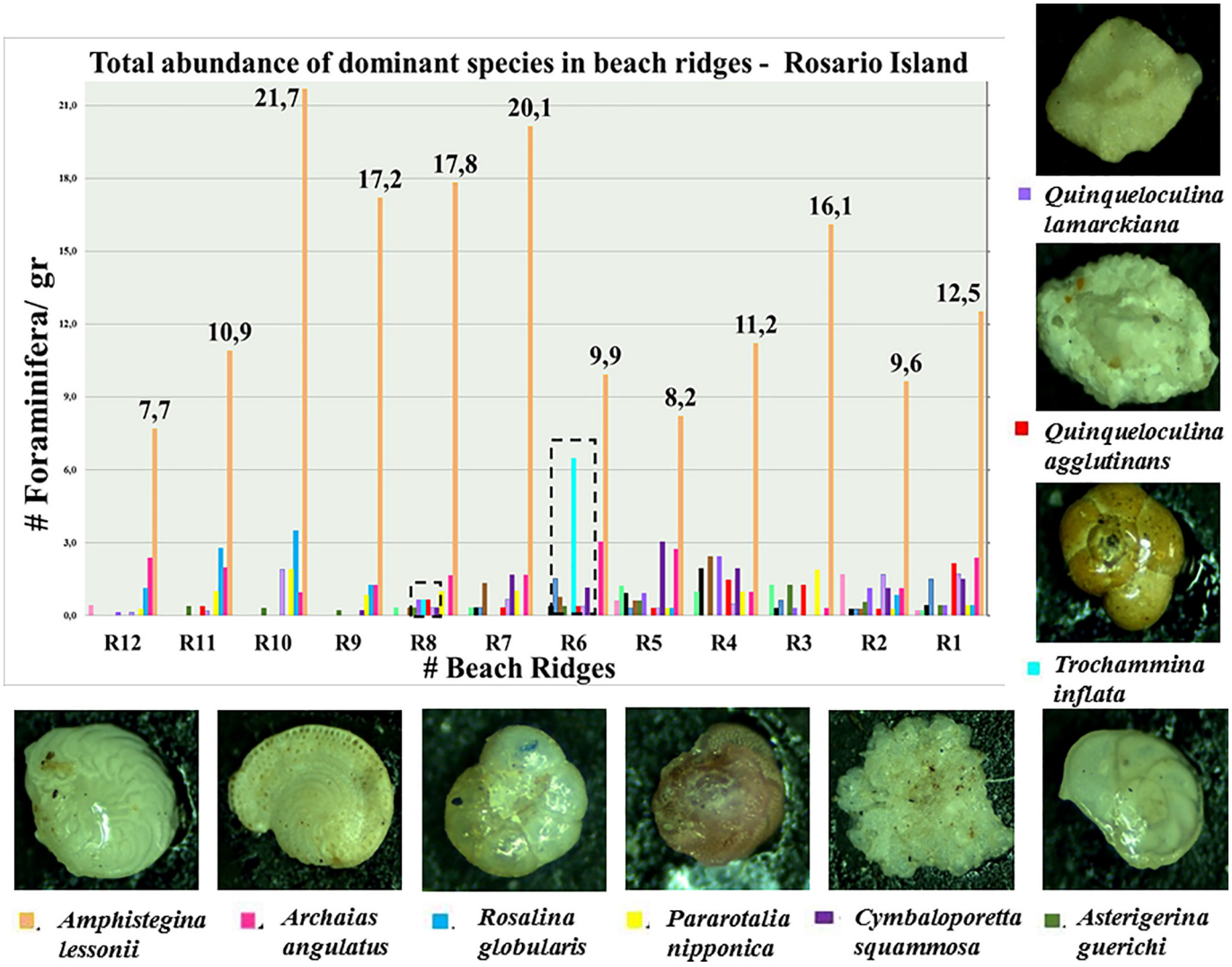

Fig. 7. Total abundance of dominant species of benthic foraminifera in the beach ridges.

diapiric event could have also produced erosional signatures in the Archipelago. Evidence for uplift and eastward tilting on Rosario Island include: (1) occurrence of terraces on the NE side of the island, but flat costal morphology on the SW side; (2) a marked difference in terrace stratigraphy, showing dissimilar strata in the east and west; (3) increasing elevation of beach level to the east, detected in the surveyed profiles. Furthermore, Vernette (1989) and Martínez et al. (2010) discussed evidence of active regional diapirism and compressional tectonics. One strong event of this type was the 1834 earthquake, with the epicenter in Santa Marta, Colombia. This is the only earthquake that occurred in the Colombian Caribbean within that time frame. With a magnitude 6.4 in the M_W scale and an intensity of 8 in the EMS-98 scale, this earthquake was felt in the vicinity of Cartagena (Ramirez, 1975; Servicio Geológico Colombiano, http: http://sish.sgc.gov.co/visor/sesionServlet?metodo=irAIntensidadesSismo&idSismo=4).

5.3. Further considerations

The LP2 core possesses no evidence of terrigenous supply from construction of the El Dique Channel. The El Dique Channel was opened in 1650 from the Magdalena River (Mogollon-Vélez, 2013), the river with the greatest sediment discharge to the Caribbean. After El Dique construction, significant volumes of sediment started to reach Cartagena Bay. There have been a number of recent modifications to the channel, especially in 1952 and 1984, which increased sediment discharge that reached the ERIA (Moreno-Madriñán et al., 2015). In the LP2 core, terrigenous content is very similar in units 1 through 3, prior to 1655, but decreases considerably in the uppermost section. Lack of evidence for increased sediment supply from the El Dique Channel can be attributed to the ongoing resuspension of fine sediment in the Archipelago under prevailing, relatively high-energy oceanic conditions.

Finally, given that extreme oceanic events in the El Rosario Islands have shaped coastal morphology and influenced reef lagoon sedimentation, it can be expected that future extremes, associated with global climate change, will be related to landscape changes and consequent sediment supply to the reefs. According to the IPCC (2014), there is low confidence in wave height predictions, but it is very likely that mean sea level rise will contribute to upward trends in coastal, extreme high water levels in the future. There is, however, significant confidence that locations currently experiencing coastal erosion and flooding will continue to do so in the future as a consequence of increasing sea level. Furthermore, both mean tropical cyclone maximum wind speed and frequency of stronger hurricanes are likely to increase. If the main tracks of tropical storms change because of changes in sea surface temperature in the Colombian Basin, hurricane dynamics could have greater impact on regions of the Colombian coast, including the El Rosario Archipelago.

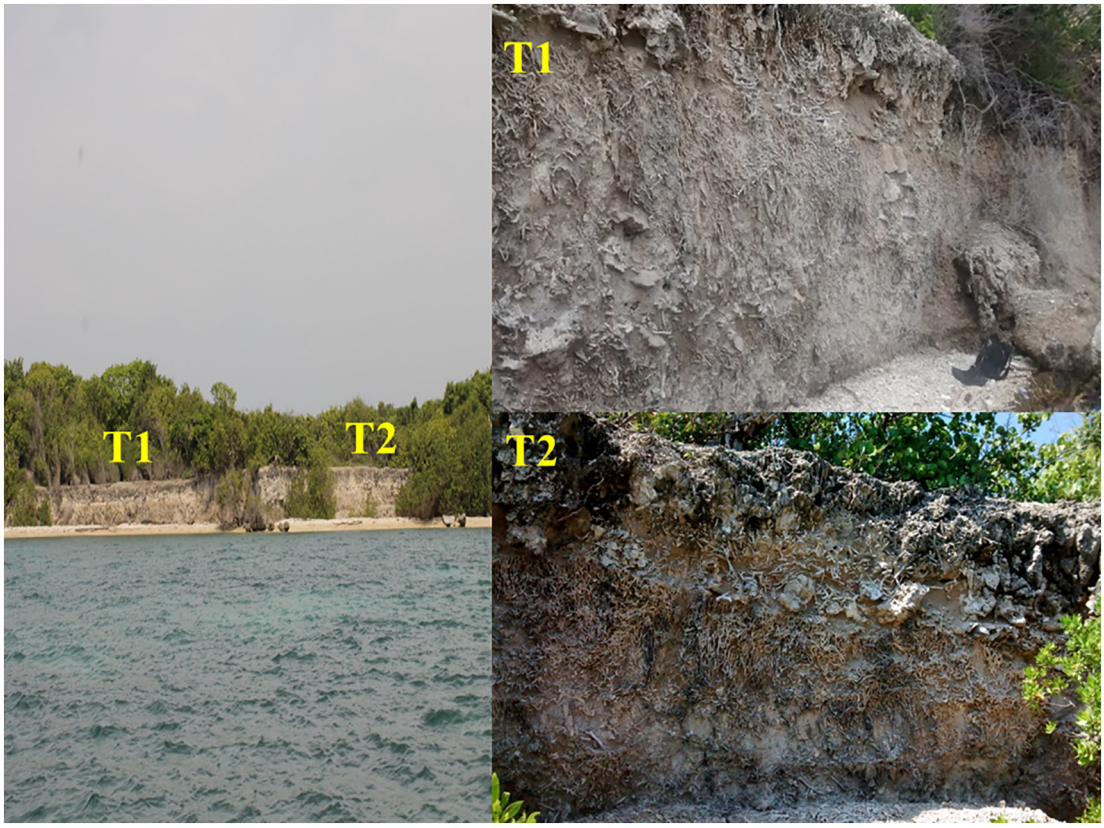

Fig. 8. Ancient Terraces (T1 and T2) on southeast Rosario Island. Panoramic view of the terraces (left). Overall appearance of the terraces at the outcrop scale.

6. Conclusions

In this study we combined analyses of historical climatic-oceanographic series and sediment and microfossil records in the ERIA to understand past extreme events that occurred in this area of the Caribbean Sea and their impacts on ERIA geomorphologic processes. The strongest and longest-duration wind events around the ERIA coincided with some of the highest-wave events. Nevertheless, high-sea-level extreme events did not correspond to extreme wave events. Most of the high-wind, extreme wave events seem to have occurred during the dry season and were perhaps related to cold fronts. When they occurred during the wet season, high-energy wave events were associated with the passage of hurricanes. The strongest and longest high-sea-level events occurred during the wet season and/or under ENSO conditions. Major storms recurred at intervals of ca. 70 years and determined the formation of beach ridges on Rosario Island, where sediments eroded from neighboring terraces constitute one of the main sources of detrital material. The progression of beach ridges ultimately contributed to the closure of a small mangrove lagoon ca. 1657 CE. Sediments deposited during the last 1800 years in Pajarales Lagoon represent a 56-cm section that can be classified as high energy on the basis of grain size, gradation and age inversion. The event that formed this unit probably occurred after 1655 CE and coincided with formation of a gap between two beach ridges on Rosario Island.

Extreme wave events detected in the historical record possessed enough energy to have mobilized sediments at the bottom of the Pajarales Lagoon and suspend particles < 0.3 mm, but it is unlikely that such events produced the high energy unit. First estimates of wave heights produced by tsunamis in the region indicate they are not significantly different from wave heights generated by extreme climate events. Other potential causes of this deposit are tectonic events and diapirism. The earthquake that occurred in nearby Santa Marta in 1834 could have produced the storm-like sediments. Nevertheless, existing information is insufficient to identify unequivocally the specific event or process that gave rise to these deposits.

Our data show that events such as earthquakes and storms exert strong controls on coastal geomorphology and reef sedimentation in the ERIA. If future climate change increases the frequency and/or magnitude of major storms that impact the Caribbean coast of Colombia, the ERIA will be subject to pronounced future landscape transformations that will impact ecosystems and settlers alike.

Data availability

Oceanographic and climatic datasets related to this article come from well-known international databases cited appropriately in the Methods section. The sedimentological databases and in situ measurements can be found at http://siam.invemar.org.co/, the system of environmental marine information of Colombia, hosted by Invemar.

Acknowledgments

This research was carried out under the project “Extreme events in insular ecosystems of the Caribbean and Colombian Pacific” sponsored by the National University of Colombia and COLCIENCIAS (1118-569-34826). Support for ^{210}Pb dating came from the University of Florida's Land Use and Environmental Change Institute (LUECI).

References

Almogi-Labin, A., Siman-Tov, R., Rosenfeld, A., Debard, E., 1995. Occurrence and distribution of the foraminifer Ammonia beccarii tepida (Cushman) in water bodies, recent and quaternary, of the Dead Sea rift, Israel. Mar. Micropaleontol. 26 (95): 153–159. https://doi.org/10.1016/0377-8398(95)00013-5.

Amador, J., 2008. The intra-Americas sea low-level jet: overview and future research. Ann. N. Y. Acad. Sci. 1146 (1):153–188. https://doi.org/10.1196/annals.1446.012.

Andrade, C.A., Barton, E.D., 2000. Eddy development and motion in the Caribbean Sea. J. Geophys. Res. 105, 191–201.

Appleby, P.G., Oldield, F., 1983. The assessment of 210Pb data from sites with varying sediment accumulation rates. Hydrobiologia 103:29–35. https://doi.org/10.1007/BF00028424.

Beier, E., Bernal, G., Ruiz-Ochoa, M., Barton, E.D., 2017. Freshwater exchanges and surface salinity in the Colombian basin, Caribbean Sea. PLoS One 12 (8), e0182116. https://doi.org/10.1371/journal.pone.0182116.

Bendixen, M., Clemmensen, L.B., Kroon, A., 2013. Sandy berm and beach-ridge formation in relation to extreme sea-levels: a Danish example in a micro-tidal environment. Mar. Geol. 344:53–64. https://doi.org/10.1016/j.margeo.2013.07.006.

Bernal, G., Ruiz-Ochoa, M., Beier, E., 2010. Variabilidad estacional e interanual océano atmósfera en la cuenca Colombia. In: Campos, N.H., Acero, A., Mancera, J.E. (Eds.), La investigación en Ciencias del Mar de la Universidad Nacional de Colombia. 30 años de la Biología Marina. 14. Universidad Nacional de Colombia, Bogotá. Cuadernos del Caribe, pp. 49–72.

Bernal, G., Osorio, A.F., Urrego, L., Pelaez, D., Molina, E., Zea, S., Montoya, R.D., Villegas, N., 2016. Occurrence of energetic extreme oceanic events in the Colombian Caribbean coasts and some approaches to assess their impact on ecosystems. J. Mar. Syst. 164: 85–100. https://doi.org/10.1016/j.jmarsys.2016.08.007.

Binford, M.W., 1990. Calculation and uncertainty of 210Pb dates for PIRLA project sediment cores. J. Paleolimnol. 3:253–267. https://doi.org/10.1007/BF00219461.

Blake, E.S., Kimberlain, T.B., Berg, R.J., Cangialosi, J.P., Beven, J.L., 2013. Tropical cyclone report hurricane sandy. J. Chem. Inf. Model. 53:1689–1699. https://doi.org/10.1017/CBO9781107415324.004.

Boltovskoy, E., Wright, E., 1976. Recent Foraminifera. Springer, Netherlands.

Bourrouilh, F.G., Beck, C., Gorsline, D.S., 2007. Catastrophic events (hurricanes, tsunami and others) and their sedimentary records: introductory notes and new concepts for shallow water deposits. Sediment. Geol. 199:1–11. https://doi.org/10.1016/j.sedgeo.2006.12.007.

Braun, E., Meyer, B., Deocampo, D., Kiage, L.M., 2017. A 3000 yr paleostorm record from St. Catherines Island, Georgia. Estuar. Coast. Shelf Sci. 196:360–372. https://doi.org/10.1016/j.ecss.2017.05.021.

Brill, D., Bruckner, H., Jankaew, K., Kelletat, D., Scheffers, A., Scheffers, S., 2011. Potential predecessors of the 2004 Indian Ocean tsunami - sedimentary evidence of extreme wave events at Ban Bang Sak, SW Thailand. Sediment. Geol. 239 (3–4):146–161. https://doi.org/10.1016/j.sedgeo.2011.06.008.

Caicedo, J., Martinelli, B., Meyer, H., Steer, R., 1996. Efecto de tsunami del mar caribe en la costa de Colombia. Alerta Tsunami-Modelamiento, Corporación OSSO, pp. 1–13.

Caldwell, P.C., Merrifield, M.A., Thompson, P.R., 2015. Sea Level Measured by Tide Gauges from Global Oceans — The Joint Archive for Sea Level Holdings (NCEI Accession 0019568), Version 5.5. NOAA National Centers for Environmental Information https://doi.org/10.7289/V5V40S7W (Dataset).

Cendales, M.H., Zea, S., Díaz, J.M., 2002. Geomorfología y Unidades Ecológicas del Complejo de Arrecifes de las Islas del Rosario e Isla Barú (Mar Caribe, Colombia). Rev. Acad. Colomb. Cient. XXVI (101), 497–510.

Clemmensen, L.B., Nielsen, L., 2010. Internal architecture of a raised beach ridge system (Anholt, Denmark) resolved by ground-penetrating radar investigations. Sediment. Geol. 223 (3–4):281–290. https://doi.org/10.1016/j.sedgeo.2009.11.014.

Coco, G., Senechal, N., Rejas, a., Bryan, K.R., Capo, S., Parisot, J.P., MacMahan, J.H.M., 2014. Beach response to a sequence of extreme storms. Geomorphology 204:493–501. https://doi.org/10.1016/j.geomorph.2013.08.028.

Darrel, N., Sommers, L., 1996. Total carbon, organic carbon, and organic matter. In: Bartels, J.M. (Ed.), Methods of Soil Analysis. Soil Science Society of America, Inc.

Dee, D.P., Uppala, S.M., Simmons, a.J., Berrisford, P., Poli, P., Kobayashi, S., Vitart, F., 2011. The ERA-interim reanalysis: configuration and performance of the data assimilation system. Q. J. R. Meteorol. Soc. 137:553–597. https://doi.org/10.1002/qj.828.

Devis-Morales, A., Montoya-Sánchez, R., Bernal, G., Osorio, A.F., 2017. Assessment of extreme wind and waves in the Colombian Caribbean Sea for offshore applications. Appl. Ocean Res. 69:10–26. https://doi.org/10.1016/j.apor.2017.09.012.

Díaz, J.M., Barrios, L.M., Cendales, M.H., Garzón, J., Geister, J., López, M., Ospina, G., Parra, E., Pinzón, J., Vargas, B., Zapata, E.A., Zea, S., 2000. Áreas Coralinas de Colombia. 5. INVEMAR, Serie Publicaciones Especiales, Santa Marta.

Easterling, D.R., Meehl, G.A., Parmesan, C., Changnon, S.A., Karl, T.R., Mearns, L.O., 2000. Climate extremes: observations, modeling, and impacts. Science's Compass. 289: pp. 2068–2074. https://doi.org/10.1126/science.289.5487.2068.

Ebi, K.L., Bowen, K., 2016. Extreme events as sources of health vulnerability: drought as an example. Weather Clim. Extremes 11:95–102. https://doi.org/10.1016/j.wace.2015.10.001.

Ellis, B.F., Messina, A., 1940–2014. Catalogue of Foraminifera. Micropaleontology Press, American Museum of Natural History, New York.

Enfield, D.B., Mestas, A.M., Mayer, D.A., Cid-Serrano, L., 1999. How ubiquitous is the dipole relationship in tropical Atlantic sea surface temperatures? J. Geophys. Res. 104: 7841–7848. https://doi.org/10.1029/1998JC900109.

Fatela, F., Taborda, R., 2002. Confidence limits of species proportions in microfossil assemblages. Mar. Micropaleontol. 45 (2):169–174. https://doi.org/10.1016/S0377-8398(02)00021-X.

Forsyth, A.J., Nott, J., Bateman, M.D., 2010. Beach ridge plain evidence of a variable Late-Holocene tropical cyclone climate, North Queensland, Australia. Palaeogeogr. Palaeoclimatol. Palaeoecol. 297 (3–4):707–716. https://doi.org/10.1016/j.palaeo.2010.09.024.

Galeano, A., Urrego, L.E., Botero, V., Bernal, G., 2017. Mangrove resilience to climate extreme events in a Colombian Caribbean Island. Wetl. Ecol. Manag. 25:743–760. https://doi.org/10.1007/s11273-017-9548-9.

Gaucher, G., 1971. Tratado de pedología agrícola. Omega, Barcelona, España.

Guiney, J.L., 2000. Preliminary Report: Hurricane Lenny (1999). National Hurricane Center www.nhc.noaa.gov/1999lenny.html, Accessed date: 27 August 2008.

Hawkes, A.D., Horton, B.P., 2012. Sedimentary record of storm deposits from Hurricane Ike, Galveston and San Luis Islands, Texas. Geomorphology 171–172:180–189. https://doi.org/10.1016/j.geomorph.2012.05.017.

Hawkes, A.D., Bird, M., Cowie, S., Grundy-Warr, C., Horton, B.P., Shau Hwai, A.T., Aik, L.W., 2007. Sediments deposited by the 2004 Indian Ocean Tsunami along the Malaysia–Thailand Peninsula. Mar. Geol. 242 (1–3):169–190. https://doi.org/10.1016/j.margeo.2007.02.017.

Hayne, M., Chappell, J., 2001. Cyclone frequency during the last 5000 years at Curacoa Island, North Queensland, Australia. Palaeogeogr. Palaeoclimatol. Palaeoecol. 168 (3–4):207–219. https://doi.org/10.1016/S0031-0182(00)00217-0.

Holthuijsen, L.H., 2007. Waves in Oceanic and Coastal Waters. Cambridge University Press, N.Y.

Houser, C., Hapke, C., Hamilton, S., 2008. Controls on coastal dune morphology, shoreline erosion and barrier island response to extreme storms. Geomorphology 100: 223–240. https://doi.org/10.1016/j.geomorph.2007.12.007.

Houser, C., Wernette, P., Rentschlar, E., Jones, H., Hammond, B., Trimble, S., 2015. Post-storm beach and dune recovery: implications for barrier island resilience. Geomorphology 234:54–63. https://doi.org/10.1016/j.geomorph.2014.12.044.

IPCC, 2014. Summary for policymakers. In: Field, C.B., Barros, V.R., Dokken, D.J., Mach, K.J., Mastrandrea, M.D., Bilir, T.E., Chatterjee, M., Ebi, K.L., Estrada, Y.O., Genova, R.C., Girma, B., Kissel, E.S., Levy, A.N., MacCracken, S., Mastrandrea, P.R., White, L.L. (Eds.), Climate Change 2014: Impacts, Adaptation, and Vulnerability. Part A: Global and Sectoral Aspects. Contribution of Working Group II to the Fifth Assessment Report of the Intergovernmental Panel on Climate Change. Cambridge University Press, Cambridge, United Kingdom and New York, NY, USA, pp. 1–32.

Jentsch, A., Kreyling, J., Beierkuhnlein, C., 2007. A new generation of climate change experiments: events, not trends. Front. Ecol. Environ. 5:365–374. https://doi.org/10.1890/1540-9295(2007)5[365:ANGOCE]2.0.CO;2.

Klostermann, L., Gischler, E., Storz, D., Hudson, J.H., 2014. Sedimentary record of Late Holocene event beds in a mid-ocean atoll lagoon, Maldives, Indian Ocean: potential for deposition by tsunamis. Mar. Geol. 348:37–43. https://doi.org/10.1016/j.margeo.2013.11.014.

Lander, J.F., Whiteside, L.S., Lockridge, P.A., 2007. A brief history of Tsunamis in the Caribbean Sea. Int. J. Tsunami Soc. 20 (2), 57–94.

Leadbetter, M., 1991. On a basis for 'peaks over threshold' modeling. Stat. Probab. Lett. 12 (4), 357–362.

Loeblich, A.R., Tappan, H., 1988. Foraminiferal Genera and Their Classification. Springer, New York.

Martínez, J.I., Yokoyama, Y., Gomez, A., Delgado, A., Matsuzaki, H., Rendon, E., 2010. Late Holocene marine terraces of the Cartagena region, southern Caribbean: the product of neotectonism or a former high stand in sea-level? J. S. Am. Earth Sci. 29 (2): 214–224. https://doi.org/10.1016/j.jsames.2009.08.010.

McCulloch, I., 1977. Qualitative Observations on Recent Foraminifera Test With Emphasis on the Eastern Pacific. University of Southern California, Los Angeles.

McManus, J., 1988. Grain size determination and interpretation. In: Tucker, M. (Ed.), Techniques in Sedimentology. Blackwell Scientific Publications, pp. 63–85.

Mogollón-Vélez, J.V., 2013. El Canal del Dique. Historia de un desastre ambiental. El Áncora Editores, Bogotá.

Moreno-Madriñán, M.J., Rickman, D.L., Ogashawara, I., Irwin, D.E., Ye, J., Al-Hamdan, M.Z., 2015. Using remote sensing to monitor the influence of river discharge on watershed outlets and adjacent coral reefs: Magdalena River and Rosario Islands, Colombia. Int. J. Appl. Earth Obs. Geoinf. 38, 204–215.

Morton, R.A., Richmond, B.M., Jaffe, B.E., Gelfenbaum, G., 2008. Coarse – clast ridge complexes of the Caribbean: a preliminary basis for distinguishing tsunami and storm – wave origins. J. Sediment. Res. 78:624–637. https://doi.org/10.2110/jsr.2008.068.

Nott, J., 1997. Extremely high-energy wave deposits inside the Great Barrier Reef, Australia: determining the cause-tsunami or tropical cyclone. Mar. Geol. 141: 193–207. https://doi.org/10.1016/S0025-3227(97)00063-7.

Nott, J., 2004. Palaeotempestology: the study of prehistoric tropical cyclones - a review and implications for hazard assessment. Environ. Int. 30:433–447. https://doi.org/10.1016/j.envint.2003.09.010.

Nott, J., 2011. A 6000 year tropical cyclone record from Western Australia. Quat. Sci. Rev. 30 (5–6):713–722. https://doi.org/10.1016/j.quascirev.2010.12.004.

Nott, J., Forsyth, A., Rhodes, E., O'Grady, D., 2015. The origin of centennial to millennial scale chronological gaps in storm emplaced beach ridge plains. Mar. Geol. 367: 83–93. https://doi.org/10.1016/j.margeo.2015.05.011.

Oldfield, F., Appleby, P.G., 1984. Empirical testing of 210Pb-dating models for lake sediments. In: Haworth, E.Y., Lund, W.G. (Eds.), Lake Sediments and Environmental History. University of Minnesota Press, Minneapolis, MN, pp. 93–124.

Ortiz-Royero, J.C., 2007. Huracanes y tormentas tropicales en el Mar Caribe colombiano desde 1900. Bol. Cient. CIOH 60 (25), 54–60.

Ortiz-Royero, J.C., Otero, L.J., Restrepo, J.C., Ruiz, J., Cadena, M., 2013. Cold fronts in the Colombian Caribbean Sea and their relationship to extreme wave events. Nat. Hazards Earth Syst. Sci. 13 (11):2797–2804. https://doi.org/10.5194/nhess-13-2797-2013.

Otvos, E.G., 2000. Beach ridges — definitions and significance. Geomorphology 32:83–108. https://doi.org/10.1016/S0169-555X(99)00075-6.

Pilarczyk, J.E., Horton, B.P., Witter, R.C., Vane, C.H., Chagué-Goff, C., Goff, J., 2012. Sedimentary and foraminiferal evidence of the 2011 Tōhoku-oki tsunami on the Sendai coastal plain, Japan. Sediment. Geol. 282:78–89. https://doi.org/10.1016/j.sedgeo.2012.08.011.

Poveda, G., Waylen, P.R., Pulwarty, R.S., 2006. Annual and inter-annual variability of the present climate in northern South America and southern Mesoamerica. Palaeogeogr. Palaeoclimatol. Palaeoecol. 234 (1):3–27. https://doi.org/10.1016/j.palaeo.2005.10.031.

Puerres, L.Y., 2016. Indicadores sedimentológicos de Eventos oceánicos energéticos extremos en el Parque Nacional Natural Islas del Rosario. (MSc Tesis). Universidad Nacional de Colombia, Medellín.

Ramirez, J.E., 1975. Historia de los terremotos en Colombia. Instituto Geográfico Agustín Codazzi, Colombia.

Reimer, P.J., Bard, E., Bayliss, A., Beck, J.W., Blackwell, P.G., Bronk Ramsey, C., Buck, C.E., Cheng, H., Edwards, R.L., Friedrich, M., Grootes, P.M., Guilderson, T.P., Haflidason, H., Hajdas, I., Hatté, C., Heaton, T.J., Hoffmann, D.L., Hogg, A.G., Hughen, K.A., Kaiser, K.F., Kromer, B., Manning, S.W., Niu, M., Reimer, R.W., Richards, D.A., Scott, E.M., Southon, J.R., Staff R.A, Turney, C.S.M., Van der Plicht, J., 2013. IntCal13 and Marine13 radiocarbon age calibration curves 0–50,000 years cal BP. Radiocarbon 55 (4), 1869–1887.

Restrepo, J.C., Otero, L., Casas, A.C., Henao, A., Gutiérrez, J., 2012. Shoreline changes between 1954 and 2007 in the marine protected area of the Rosario Island Archipelago (Caribbean of Colombia). Ocean Coast. Manag. 69:133–142. https://doi.org/10.1016/j.ocecoaman.2012.07.027.

Restrepo, J.C., Franco, D., Escobar, J., Correa, I.D., Otero, L., Gutiérrez, J., 2013. Bahía de Cartagena (Colombia): distribución de sedimentos superficiales y ambientes sedimentarios. Lat. Am. J. Aquat. Res. 41 (1), 99–112 (doi: 103856/vol41-issue1-fulltext-8).

Restrepo, J.D., Park, E., Aquino, S., Latrubesse, E.M., 2016. Coral reefs chronically exposed to river sediment plumes in the southwestern Caribbean: Rosario Islands, Colombia. Sci. Total Environ. 553:316–329. https://doi.org/10.1016/j.scitotenv.2016.02.140.

Robbins, J.A., 1978. Geochemical and geophysical applications of radioactive lead isotopes. In: Nriago, J.P. (Ed.), Biogeochemistry of Lead. North Holland, Amsterdam, pp. 285–393.

Roelvink, D., van Dongeren, A., McCall, R., Hoonhout, B., van Rooijen, A., van Geer, P., de Vet, L., Nederhoff, K., Quataert, E., 2015. XBeach Technical Reference: Kingsday Release. :pp. 1–141 https://doi.org/10.13140/RG.2.1.4025.6244.

Ruiz Ochoa, M., Beier, E., Bernal, G., Barton, E.D., 2012. Sea surface temperature variability in the Colombian Basin, Caribbean Sea. Deep-Sea Res. I 64:43–53. https://doi.org/10.1016/j.dsr.2012.01.013.

Scheffers, S.R., Haviser, J., Browne, T., Scheffers, A., 2009. Tsunamis, hurricanes, the demise of coral reefs and shifts in prehistoric human populations in the Caribbean. Quat. Int. 195 (1–2):69–87. https://doi.org/10.1016/j.quaint.2008.07.016.

Schelske, C.L., Peplow, A., Brenner, M., Spencer, C.N., 1994. Low-background gamma counting: applications for 210Pb dating of sediments. J. Paleolimnol. 10, 115–128.

Sen Gupta, B., 1999. Modern Foraminifera. Kluwer Academic Publishers, Dordrecht.

Sura, P., 2011. A general perspective of extreme events in weather and climate. Atmos. Res. 101 (1–2):1–21. https://doi.org/10.1016/j.atmosres.2011.01.012.

Talma, A.S., Vogel, J.C., 1993. Radiocarbon 35 (2), 317–322.

Tamura, T., 2012. Beach ridges and prograded beach deposits as palaeoenvironment records. Earth-Sci. Rev. 114 (3–4):279–297. https://doi.org/10.1016/j.earscirev.2012.06.004.

Tanner, W.F., 1995. Origin of beach ridges and swales. Science 129, 149–161.

Tomczak, M., Godfrey, J., 1994. Regional Oceanography: An Introduction. Elsevier Science, Oxford.

Torres, R.R., Tsimplis, M.N., 2014. Sea level extremes in the Caribbean Sea. J. Geophys. Res. Oceans Atmos. 119:4714–4731. https://doi.org/10.1002/2014JC009929.

Vernette, J.G., 1978. Cartografía de los fondos en la plataforma continental: estandarización de los crite- rios sedimentológicos. Bol. Cient. CIOH 4, 3–13.

Vernette, G., 1989. Examples of diapiric control on shelf to pography and sedimentation patterns on the Colombian Caribbean continental shelf. J. S. Am. Earth Sci. 2 (4), 391–400.

Yandar, M.A., De la Cruz, R.A., 2015. Aproximación numérica a la propagación de ondas de tsunami y caso de estudio en la costa Caribe Colombiana. Bol. Mat. 22 (2), 135–149.